Molecular etiology of a dominant form of type III hyperlipoproteinemia caused by R142C substitution in apoE4[S]

Alexander M. Vezeridis, Konstantinos Drosatos,[1] and Vassilis I. Zannis[2]

Molecular Genetics, Whitaker Cardiovascular Institute, Boston University School of Medicine, Boston MA

Abstract **We have used adenovirus-mediated gene transfer in apolipoprotein (apo)$E^{-/-}$ mice to elucidate the molecular etiology of a dominant form of type III hyperlipoproteinemia (HLP) caused by the R142C substitution in apoE4. It was found that low doses of adenovirus expressing apoE4 cleared cholesterol, whereas comparable doses of apoE4[R142C] greatly increased plasma cholesterol, triglyceride, and apoE levels, caused accumulation of apoE in VLDL/IDL/LDL region, and promoted the formation of discoidal HDL. Co-expression of apoE4[R142C] with lecithin cholesterol acyltransferase (LCAT) or lipoprotein lipase (LPL) in $apoE^{-/-}$ mice partially corrected the apoE4[R142C]-induced dyslipidemia. High doses of C-terminally truncated apoE4[R142C]-202 partially cleared cholesterol in $apoE^{-/-}$ mice and promoted formation of discoidal HDL. The findings establish that apoE4[R142C] causes accumulation of apoE in VLDL/IDL/LDL region and affects in vivo the activity of LCAT and LPL, the maturation of HDL, and the clearance of triglyceride-rich lipoproteins.[FLR] The prevention of apoE4[R142C]-induced dyslipidemia by deletion of the 203-299 residues suggests that, in the full-length protein, the R142C substitution may have altered the conformation of apoE bound to VLDL/IDL/LDL in ways that prevent triglyceride hydrolysis, cholesterol esterification, and receptor-mediated clearance in vivo.**—Vezeridis, A. M., K. Drosatos, and V. I. Zannis. **Molecular etiology of a dominant form of type III hyperlipoproteinemia caused by R142C substitution in apoE4.** ***J. Lipid Res.*** **2011.** 52: **45–56.**

Supplementary key words apolipoprotein E • lipoprotein lipase • lecithin:cholesterol acyl transferase • hypertriglyceridemia • recombinant adenovirus • gene transfer

Apolipoprotein E (apoE) is a very important protein of the lipoprotein transport system. It is required for the clearance of lipoprotein remnants from the circulation and is essential for atheroprotection (1–3).

Lipoprotein-bound apoE is the ligand for the LDL receptor as well as other receptors in vitro (4–6). In vivo and in vitro studies have shown that mutations in apoE that diminish binding of apoE-containing lipoproteins to the LDL receptor are associated with high plasma cholesterol levels and cause premature atherosclerosis in humans and experimental animals (1–3, 7, 8). Most recently we have shown that apoE is involved in the biogenesis of distinct apoE-containing HDL species with the participation of the ABCA1 lipid transporter and lecithin cholesterol acyltransferase (LCAT) (9).

Certain apoE phenotypes and genotypes are associated with recessive or dominant forms of type III hyperlipoproteinemia (HLP). The recessive form of type III HLP is encountered in subjects with the E2/2 phenotype which results from the substitution of Cys for Arg-158 (10). This mutation combined with other genetic or environmental factors affects the catabolism of apoE-containing lipoproteins and results in the accumulation in plasma of remnants of lipoprotein catabolism (7, 11). A variety of rare mutations in the 136-147 region of apoE are associated with a dominant mode of inheritance of type III HLP that is expressed at an early age (7, 8, 12, 13). The degree of penetrance of the disease varies depending on the mutation (7).

In the present study we investigated the molecular etiology of a dominant form of type III HLP caused by the R142C substitution in apoE4. Using adenovirus-mediated gene transfer in $apoE^{-/-}$ mice, we show that compared with wild-type (WT) apoE4, the apoE4[R142C]

This work was supported by a grant from the National Institutes of Health (HL68216). A. Vezeridis was supported by the National Institutes of Health Predoctoral Training Grant (HL007969). Its contents are solely the responsibility of the authors and do not necessarily represent the official views of the National Institutes of Health. Note: This information was not included in the initial versions of the online and print article but has been added in the online version after print publication.

Manuscript received 12 May 2010 and in revised form 21 September 2010.

Published, JLR Papers in Press, September 22, 2010
DOI 10.1194/jlr.M008409

Abbreviations: ApoE, apolipoprotein E; CE, cholesterol ester; EM, electron microscopy; FPLC, fast-protein liquid chromatography; GFP, green fluorescent protein; HLP, hyperlipoproteinemia; LCAT, lecithin cholesterol acyltransferase; pfu, plaque-forming unit; TC, total cholesterol; WT, wild-type

[1]Present address of K. Drosatos: Columbia University School of Medicine, College of Physicians and Surgeons, Division of Preventive Medicine and Nutrition, New York, NY.

[2]To whom correspondence should be addressed.
e-mail: vzannis@bu.edu

[S] The online version of this article (available at http://www.jlr.org) contains supplementary data in the form of two figures.

mutant dramatically increased plasma cholesterol, triglyceride, and apoE levels; decreased esterification of cholesterol in all lipoprotein fractions; promoted formation of discoidal HDL; and caused accumulation of apoE, mostly in the VLDL/IDL/LDL region. Despite the abundance of apoE in the VLDL/IDL/LDL, these lipoprotein particles cannot be processed properly by lipoprotein lipase (LPL) and LCAT and cannot be catabolized directly by the LDL receptor. The observed dyslipidemia can be partially corrected by treatment with LPL or LCAT and is prevented by deletion of the C-terminal domain of the mutant apoE.

MATERIALS AND METHODS

Materials

Materials not mentioned in this section have been obtained from sources described previously (14, 15).

Recombinant adenovirus construction

The recombinant adenoviruses were constructed as described using the Ad-Easy-1 system where the adenovirus construct is generated in BJ-5183 bacterial cells (16, 17). Following large-scale infection of HEK 293 cell cultures, the recombinant adenoviruses were purified by two consecutive $CsCl_2$ ultracentrifugation steps, dialyzed, and titrated. Usually, titers of approximately 2–5 × 10^{10} pfu/ml were obtained.

Animal studies, RNA isolation, and apoE mRNA quantitation

Male and female apoE-deficient mice 8–10 weeks old were used in these studies. Groups of four or more mice were injected intravenously through the tail vein with a dose of 0.5-3.5 × 10^9 pfu of adenoviruses expressing WT and truncated human apoE forms. Blood was obtained from the tail vein after a 4 h fast preceding adenoviral injection and on days 1, 2, 3 and 4 postinfection. The plasma was isolated and stored at 4°C and −20°C. Four or more animals from each group were euthanized four days postinfection, hepatic RNA was isolated by the triazol method, and apoE mRNA levels were determined by quantitative PCR using the standard TaqMan thermal cycling program and Applied Biosystems probe sets for human apoE and 18s rRNA (Cat. #HJ00171168-M1 and 4319413E, respectively).

Fast-protein liquid chromatography fractionation and plasma lipid and apoE determination

For fast-protein liquid chromatography (FPLC) analysis of plasma samples, 12 μl of plasma were diluted 1:4 with PBS, loaded onto a Superose 6 column in a SMART micro FPLC system (Pharmacia), eluted with PBS. A total of 25 fractions of 50 μl volume each were collected for further analysis. Triglycerides and cholesterol of plasma and the FPLC fractions were determined spectrophotometrically at 540 nm and 490 nm, respectively, as described previously (16) using the Serum Triglyceride Kit (Sigma) and Thermo Infinity Cholesterol Reagent (Thermo Fisher), according to the manufacturer's instructions. Plasma apoE concentrations were determined by sandwich ELISA using apoE standards supplied by Wako Chemicals (Richmond, VA) (16).

Statistical analysis

Data are presented as mean ± SD. Statistically significant differences between two groups of mice were determined using Student's *t*-test with unequal variance.

Density gradient ultracentrifugation and electron microscopy analysis

To assess the ability of WT and truncated apoE forms to associate with different lipoproteins, an aliquot of 0.3 ml of plasma was fractionated by KBr density gradient ultracentrifugation. Ten fractions were collected and analyzed by SDS-PAGE as described previously (18, 19). Aliquots of fractions 6-8, which contain most of the apoE, obtained by density gradient ultracentrifugation, were analyzed by electron microscopy (EM). The photomicrographs were taken at 75,000× magnification and enlarged three times as described previously (20).

Non-denaturing two-dimensional electrophoresis

The distribution of HDL subfractions in plasma was analyzed by two-dimensional electrophoresis as described (19, 21). ApoE was detected by probing the membrane with a goat polyclonal anti-human apoE antibody (Meridian Biosciences K74190G; Saco, ME).

RESULTS

ApoE4[R142C] induces dyslipidemia characterized by high plasma cholesterol triglyceride and apoE levels

To elucidate how the R142C substitution in human apoE4 induces dyslipidemia, we employed adenovirus-mediated gene transfer of full-length or truncated forms of apoE4[R142C]202 or the control WT apoE4 in apoE$^{-/-}$ mice. The experiments with the truncated apoE-202 forms were designed to assess the contribution of the C-terminal domain of the mutant protein in the induction of dyslipidemia. We found that infection of apoE$^{-/-}$ mice with a low dose (5 × 10^8 pfu) of an adenovirus expressing apoE4[R142C] increased plasma cholesterol over a four-day period and induced severe hypertriglyceridemia (**Fig. 1A**, B). The increase in triglyceride levels correlated with parallel increases in plasma apoE levels (Fig. 1C). In contrast, infection of apoE$^{-/-}$ mice with a similar dose (5 × 10^8 pfu) of adenovirus expressing wild-type apoE4 cleared cholesterol, did not affect plasma triglycerides levels, and caused only a small increase in plasma apoE levels (Fig. 1A-C). Real-time qRT-PCR analysis showed that the hepatic apoE4 and apoE4[R142C] mRNA four days postinfection were not statistically different (Fig. 1D).

ApoE4[R142C]-mediated dyslipidemia affects the HDL cholesterol esterification

FPLC analysis of plasma from apoE$^{-/-}$ mice infected with 5 × 10^8 pfu of adenoviruses expressing wild-type apoE4 showed that over 85% of the cholesterol was found in HDL-sized particles and was mostly esterified (Fig. 1E). In contrast, when apoE$^{-/-}$ mice were infected with 5 × 10^8 pfu of adenoviruses expressing apoE4[R142C], the majority of cholesterol (over 90%) was distributed in the VLDL/IDL region, a small amount of cholesterol was found in HDL, and it was unesterified (Fig. 1F).

Distribution of apoE to different lipoprotein fractions following density gradient ultracentrifugation and analysis of HDL fraction by EM

To assess the distribution of apoE and other apolipoproteins within different lipoprotein fractions, plasma

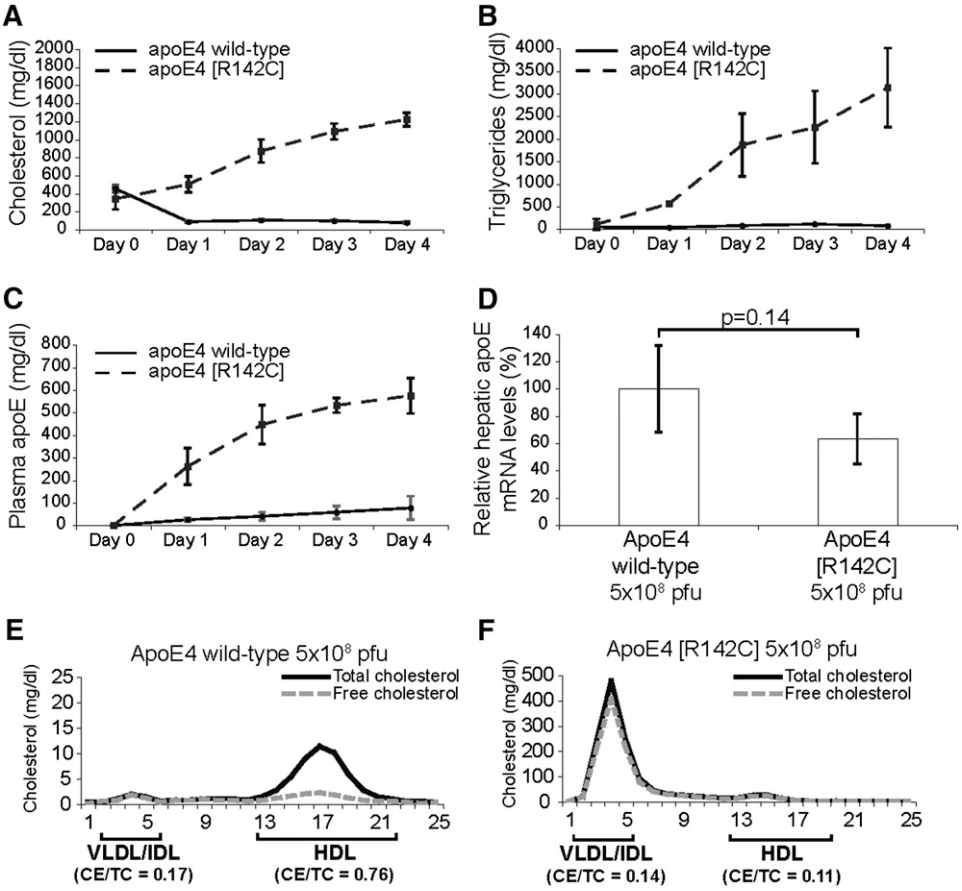

Fig. 1. Plasma cholesterol, triglycerides, apoE, apoE mRNA levels, and FPLC profiles of apoE$^{-/-}$ mice infected with 5×10^8 pfu of recombinant adenoviruses expressing the wild-type apoE4 and the apoE4[R142C] mutant on days 1 to 4 postinfection. A-D: Levels of plasma cholesterol, plasma triglycerides, plasma apoE, and hepatic human apoE mRNA. E, F: Cholesterol FPLC profiles. Total cholesterol (esterified plus unesterified) is represented by a solid black line, and free unesterified cholesterol is represented by a dashed line. The positions of the VLDL/IDL and HDL fractions and the CE/TC ratio are indicated. Parameters are mean ± SD. ApoE, apolipoprotein E; CE, cholesterol ester; FPLC, fast-protein liquid chromatography; TC, total cholesterol.

obtained four days postinfection with adenoviruses expressing the wild-type or the mutant apoE4 forms were fractionated by density gradient ultracentrifugation, and the fractions were analyzed by SDS-PAGE. When the mice were infected with a low dose of apoE4-expressing adenovirus (5×10^8 pfu), most of the apoE was found in the HDL3 region. This distribution is consistent with the formation of apoE-containing HDL as previously described (9) (**Fig. 2A**).

However, when the mice were infected with 5×10^8 pfu of adenovirus expressing apoE4[R142C] in addition to the apoE floating in the HDL3 region, there was a dramatic increase of apoE in the VLDL/IDL/LDL region as well as a shift of apoE toward the HDL2 region (Fig. 2B). Overall, there was a 7.5-fold increase of the mutant compared with the WT apoE4 in plasma. Fig. 2A and 2B also indicate that as the human apoE levels increase, the mouse apoA-I levels decrease.

Electron microscopy of fractions 6 and 7 (Fig. 2A, B), which correspond to the HDL3 region, showed that apoE$^{-/-}$ mice infected with a low dose (5×10^8 pfu) of apoE4 expressing adenovirus formed spherical HDL (Fig. 2C), whereas mice infected with a low dose (5×10^8 pfu) of apoE4[R142C] expressing adenovirus formed a mixture of spherical and discoidal HDL particles (Fig. 2D). This is consistent with the CE/TC ratios of the HDL peak observed (Fig. 1E, F).

Together, the data in Figs. 1 and 2 establish that the differences in plasma cholesterol, triglyceride, and apoE levels, the inhibition of esterification of cholesterol, and the formation of discoidal HDL are not the result of different levels of gene expression of the wild-type apoE4 and the apoE4[R142C] but, rather, reflect alterations in the properties of the apoE[R142C] mutant. To assess whether the apoE4[R142C] mutant has a dominant effect over the WT apoE we co-expressed these proteins in apoE$^{-/-}$ mice. Co-infection of E$^{-/-}$ mice with a mixture of 3.0×10^8 each of adenovirus expressing apoE4[R142C] and WT apoE3 increased plasma cholesterol levels induced severe hypertriglyceridemia and caused accumulation of apoE in the VLDL/IDL/LDL/HDL region (supplementary Fig. IA, B, D). In contrast infection with 6×10^8 pfu of the adenovirus expressing apoE3 cleared cholesterol and did not increase plasma triglyceride levels and all apoE was distributed in the HDL region (supplementary Fig. 1A-C). The findings

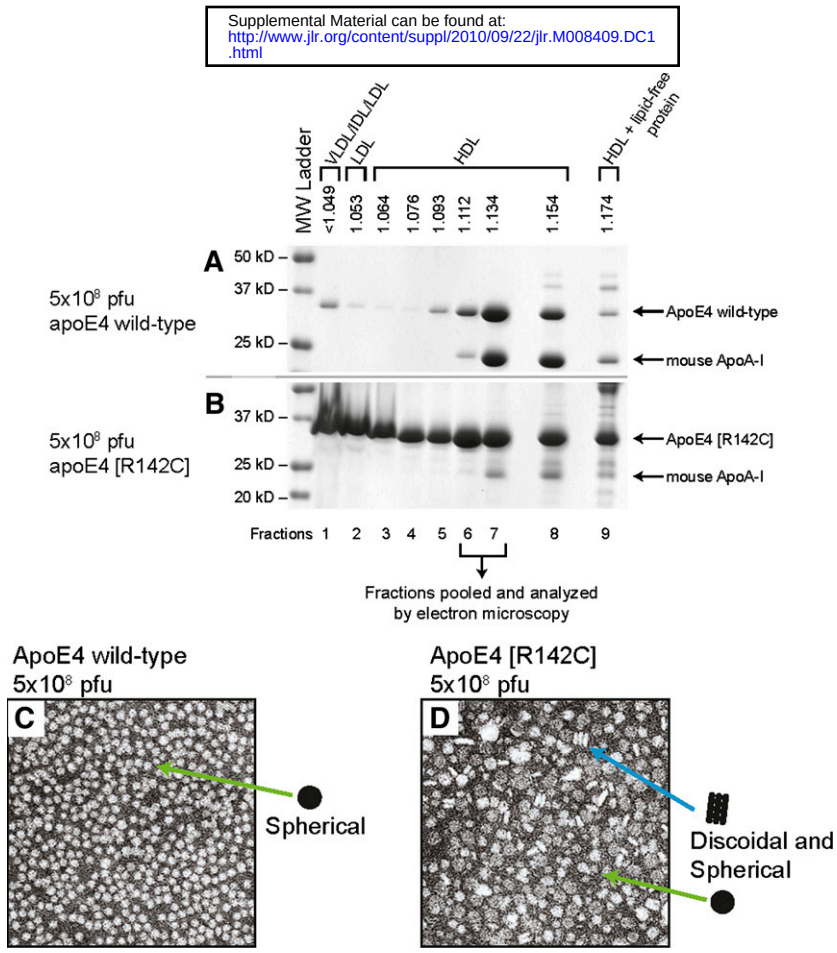

Fig. 2. Distribution of apoE in different lipoprotein fractions following density gradient ultracentrifugation of plasma and EM of the HDL fractions. A, B: Plasma samples obtained on day 4 postinfection from apoE$^{-/-}$ mice with (A) 5×10^8 pfu of apoE4 wild-type or (B) apoE4[R142C] mutant were fractionated by density gradient ultracentrifugation and analyzed by SDS-PAGE as described in "Materials and Methods." The density of each fraction and the position of apoE in the VLDL/IDL, LDL, and HDL fractions are indicated. Fractions 6 and 7 were pooled and analyzed by EM. C, D: EM analysis of HDL fractions obtained from E$^{-/-}$ mice infected with 5×10^8 adenoviruses expressing (C) apoE4 wild-type or (D) apoE4[R142C] mutant. ApoE, apolipoprotein E; EM, electron microscopy.

suggest that the mutant protein has a dominant effect in the clearance of lipoprotein remnants.

The role of LCAT in the induction of dyslipidemia in mice expressing apoE4[R142C]

The decrease in CE/TC ratio of VLDL and HDL observed (Fig. 1F) suggested inability of LCAT to esterify the cholesterol of these lipoprotein fractions. This prompted us to assess whether the apoE4[R142C]-induced dyslipidemia could be corrected by co-infection of apoE$^{-/-}$ mice with a mixture of adenoviruses expressing apoE4[R142C] and LCAT compared with apoE4[R142C] and GFP. This analysis showed that the LCAT treatment did not correct the hypercholesterolemia, on days 1–4 postinfection, of mice expressing apoE4[R142C] plus LCAT compared with mice expressing apoE4[R142C] plus GFP (**Fig. 3A**). However, the LCAT treatment significantly decreased plasma triglyceride levels and increased plasma apoE levels on days 2–4 postinfection (Fig. 3B, C).

The expression level of apoE4[R142C] four days postinfection in mice co-expressing apoE4[R142C] and GFP was higher but not significantly different than in mice co-expressing apoE4[R142C] and LCAT (Fig. 3D). The cholesterol of HDL isolated by FPLC from mice treated with adenovirus expressing apoE4[R142C] and green fluorescent protein (GFP) was unesterified (Fig. 3E), whereas the HDL cholesterol of mice treated with adenovirus expressing apoE4[R142C] and LCAT was esterified (Fig. 3F).

Density gradient ultracentrifugation of plasma and SDS-PAGE analysis of the resulting fractions (**Fig. 4A**, B) showed a shift of apoE to the VLDL/IDL/LDL region in mice expressing apoE4[R142C] and LCAT (Fig. 4B), compared with mice expressing apoE4[R142C] and GFP (Fig. 4A). Electron microscopy of HDL fractions 5 and 6 (Fig. 4A, B) showed that apoE$^{-/-}$ mice infected with adenovirus expressing apoE4[R142C] and GFP form a mixture of discoidal and spherical particles (Fig. 4C), whereas mice infected with adenovirus expressing apoE4[R142C] and LCAT form spherical particles (Fig. 4D).

The role of LPL in the induction of dyslipidemia in mice expressing apoE4[R142C]

The accumulation of triglycerides in E$^{-/-}$ mice that received the adenovirus expressing apoE4[R142C] (Fig. 1B)

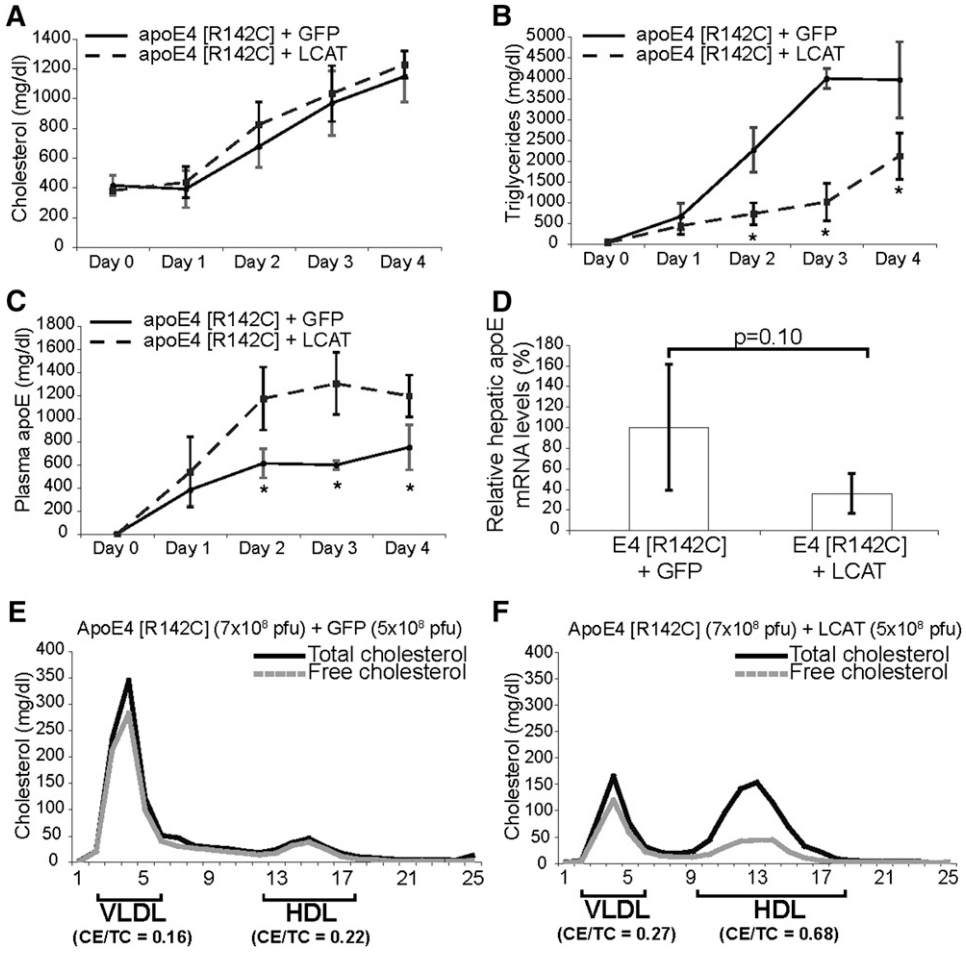

Fig. 3. Effect of LCAT on plasma lipids, plasma apoE, and hepatic apoE mRNA levels and FPLC cholesterol profiles of apoE$^{-/-}$ mice expressing apoE4[R142C]. Mice were co-infected with 7×10^8 pfu adenovirus expressing apoE4[R142C] and 5×10^8 pfu adenovirus expressing either LCAT or GFP. Plasma lipids and apoE were determined on days 0, 1, 2, 3, and 4 postinfection. Hepatic apoE mRNA levels were determined on day 4 postinfection. Data shown are mean ± SD. A-D: Levels of plasma cholesterol, plasma triglycerides, plasma apoE, and hepatic apoE mRNA. E, F: Plasma cholesterol FPLC profiles of apoE$^{-/-}$ mice co-infected with 7×10^8 pfu adenovirus expressing apoE4[R142C] and (E) 5×10^8 pfu of adenovirus expressing GFP or (F) 5×10^8 pfu of adenovirus expressing LCAT. The positions of the VLDL/IDL and HDL fractions and the CE/TC ratio are indicated. B, C: *Statistically significant difference ($P < 0.02$). ApoE, apolipoprotein E; CE, cholesterol ester; FPLC, fast-protein liquid chromatography; LCAT, lecithin cholesterol acyltransferase; TC, total cholesterol.

indicated that the endogenous lipoprotein lipase was insufficient to hydrolyze the triglycerides of VLDL. For this reason, we also assessed the ability of increased LPL to correct the dyslipidemic phenotype by co-infecting apoE$^{-/-}$ mice with a mixture of adenoviruses expressing apoE4[R142C] and LPL compared with apoE4[R142C] and GFP.

Treatment of apoE$^{-/-}$ mice with 7×10^8 pfu of adenovirus expressing apoE4[R142C] plus 5×10^8 pfu of adenovirus expressing GFP gradually increased the plasma cholesterol 2–4 days postinfection and plasma triglycerides 1–4 days postinfection, resulting in severe hypertriglyceridemia on days 2–4 postinfection (**Fig. 5A**, B).

In mice co-infected with 7×10^8 and 5×10^8 pfu, respectively, with adenovirus expressing apoE4[R142C] and LPL, cholesterol was cleared partially on day 1 and increased gradually on days 2–4 postinfection (Fig. 5A). The triglyceride levels following LPL treatment were low on day 1 but increased gradually between days 2 and 4 postinfection (Fig. 5B). However hypertriglyceridemia and hypercholesterolemia on days 2–4 was significantly decreased in mice that were co-expressing apoE4[R142C] and LPL compared with mice that were co-expressing apoE4[R142C] and GFP (Fig. 5B). Plasma apoE levels decreased significantly on day 2 following LPL treatment (Fig. 5C).

Real-time qRT-PCR analysis showed that the human apoE mRNA levels of mice co-infected with adenovirus expressing apoE4[R142C] and GFP and mice co-infected with adenoviruses expressing apoE4[R142C] and LPL were not statistically different (Fig. 5D). The HDL cholesterol of HDL isolated by FPLC from mice co-expressing apoE4[R142C] and LPL, as well as that of the control mice expressing apoE4[R142C] and GFP, was unesterified (Fig. 5E, F).

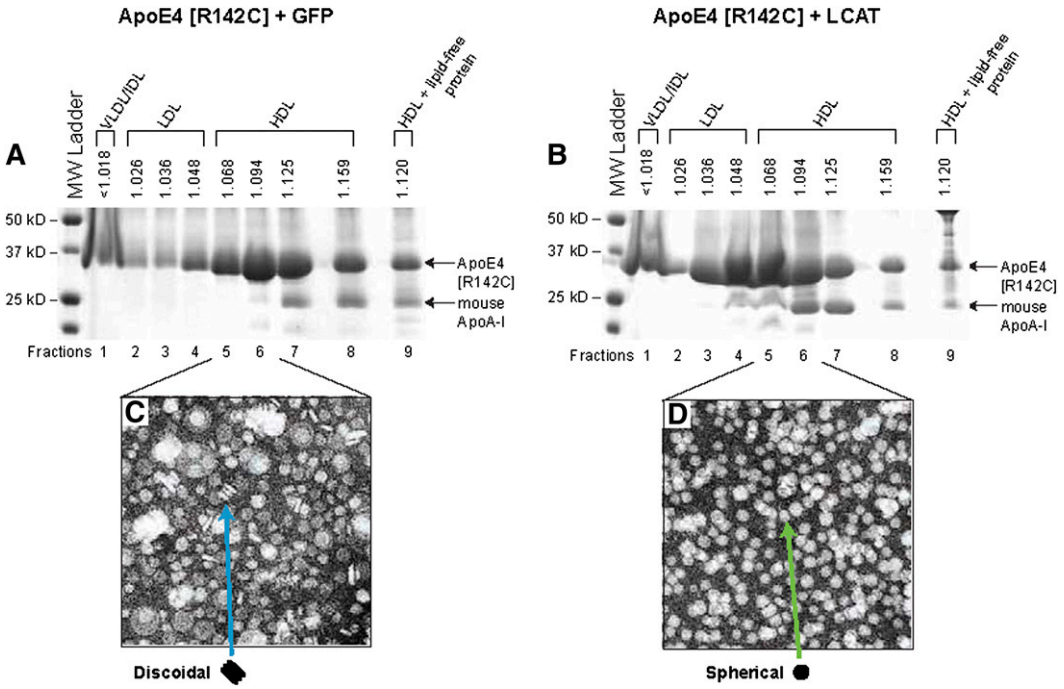

Fig. 4. Distribution of apoE in different lipoprotein fractions following density gradient ultracentrifugation of plasma and EM analysis of HDL fractions. Samples obtained from apoE$^{-/-}$ mice on day 4 postinfection with 7×10^8 pfu adenovirus expressing apoE4[R142C] and 5×10^8 pfu of adenovirus expressing either GFP or LCAT were fractionated by density gradient ultracentrifugation and analyzed by SDS-PAGE and EM as described in "Materials and Methods." The density of each fraction and the position of apoE in the VLDL/IDL, LDL, and HDL region are indicated. A, B: SDS-PAGE analysis of lipoprotein fractions obtained from mice co-infected with 7×10^8 pfu apoE4[R142C] and (A) 5×10^8 pfu GFP or (B) 5×10^8 pfu LCAT. Fractions 5 and 6 were pooled and analyzed by EM. C, D: EM analysis of samples obtained from mice infected with a mixture of adenoviruses expressing (C) apoE4[R142C] and GFP or (D) apoE4[R142C] and LCAT. ApoE, apolipoprotein E; EM, electron microscopy; LCAT, lecithin cholesterol acyltransferase.

Density gradient ultracentrifugation of the plasma of infected mice and SDS-PAGE analysis of the resulting fractions showed a reduction of the apoE levels in the VLDL/IDL/LDL region in mice expressing apoE4[R142C] and LPL, compared with mice expressing apoE4[R142C] and GFP (**Fig. 6A**, B). Electron microscopy of HDL fractions 5 and 6 (Fig. 6A, B) shows that the plasma of apoE$^{-/-}$ mice co-infected with adenovirus expressing apoE4[R142C] with either GFP or LPL contains a mixture of discoidal and spherical particles (Fig. 6C, D). This finding is consistent with the decreased CE/TC ratios observed (Fig. 5E, F).

Contribution of the C-terminal domain of apoE4[R142C] in the induction of dyslipidemia

The phenotype generated by the apoE4[R142C] mutation can be attributed exclusively to a defective recognition of the receptor-binding domain of apoE by the LDL receptor in vivo. Alternatively, additional factors brought about by interactions of the N- and C-terminal domains of the mutant apoE might contribute to the aberrant phenotype. To address this question, we performed a set of experiments using the truncated mutant apoE4[R142C]-202 form and the truncated wild-type apoE4-202 form as a control.

Treatment of apoE$^{-/-}$ mice with 2×10^9 or 3.5×10^9 pfu of adenovirus expressing apoE4[R142C]202 partially cleared cholesterol on days 1–4 postinfection and did not induce hypertriglyceridemia (**Fig. 7A**). The cholesterol levels were reduced to ~250 mg/dl on day 1 and did not change significantly on days 2–4 postinfection, indicating that apoE4[R142C]202 that lacks residues 203-299 is recognized to some extent by the LDL receptor in vivo. Consistent with previous findings (16), gene transfer of either 2 or 3.5×10^9 pfu of adenovirus expressing the WT apoE4-202 also corrected the plasma cholesterol profile of apoE$^{-/-}$ mice and did not induce hypertriglyceridemia (Fig. 7A, B).

The cholesterol levels of apoE$^{-/-}$ mice were reduced to approximately 100 mg/dl on day 1 and did not change significantly on days 2–4 postinfection (Fig. 7A, B). Triglyceride levels were in the range of 35–70 mg/dl and were not affected by the treatment with the truncated WT or mutant apoE form (data not shown).

Plasma apoE levels were significantly lower in mice expressing the WT compared with the mutant truncated apoE form (Fig. 7D). Real-time qRT-PCR analysis of human apoE mRNA showed that the hepatic human apoE mRNA levels of mice infected with 2×10^9 pfu of adenoviruses expressing apoE4[R142C]-202 or apoE4-202 were comparable (Fig. 7C). In addition, the hepatic apoE mRNA levels of mice infected with 3.5×10^9 pfu of adenoviruses expressing apoE4[R142C]-202 were lower than in mice infected with the same dose of adenoviruses expressing apoE4-202 (Fig. 7C).

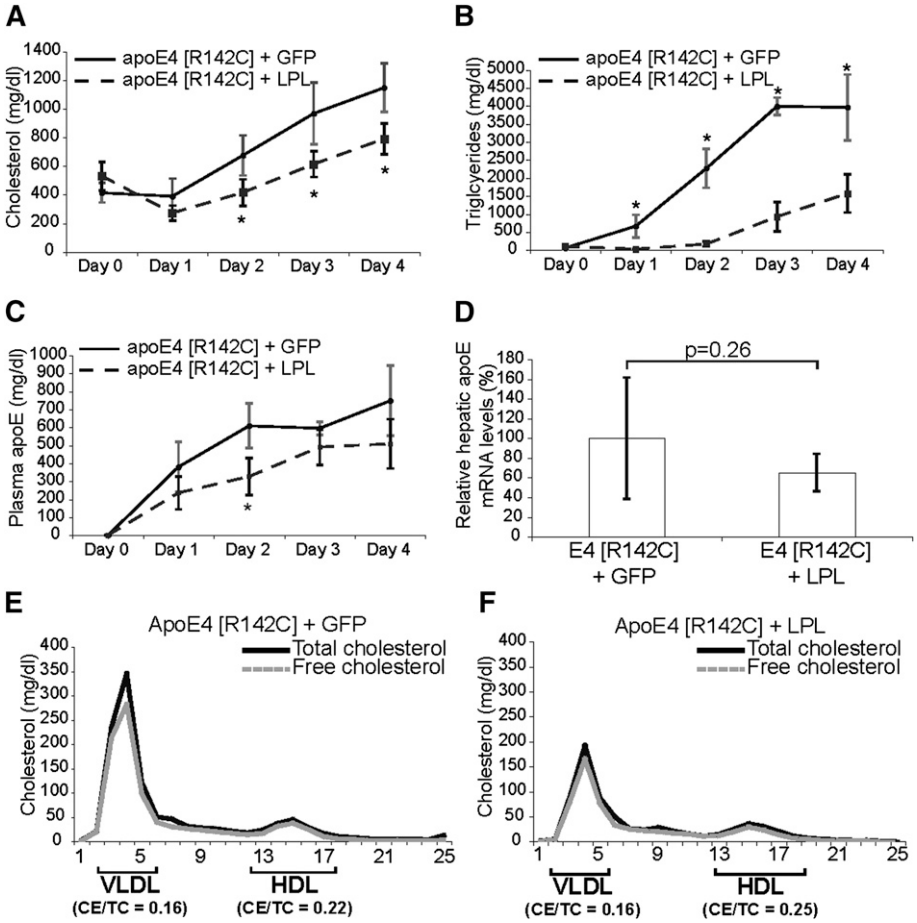

Fig. 5. Effect of LPL on plasma lipids, plasma apoE, and hepatic apoE mRNA levels of apoE$^{-/-}$ mice expressing apoE4[R142C]. Mice were co-infected with 7×10^8 pfu adenovirus expressing apoE4[R142C] and 5×10^8 pfu adenovirus expressing either LCAT or GFP. Plasma lipids and apoE levels were determined on days 0, 1, 2, 3, and 4 postinfection. Hepatic apoE mRNA levels were determined on day 4 postinfection. Data shown are expressed as mean ± SD. A-D: Levels of plasma cholesterol, plasma triglycerides, plasma apoE, and hepatic apoE mRNA. E, F: Plasma FPLC cholesterol profiles of apoE$^{-/-}$ mice co-infected with 7×10^8 pfu adenovirus expressing apoE4[R142C] and (E) 5×10^8 pfu of adenovirus expressing GFP or (F) 5×10^8 pfu of adenovirus expressing LPL. The positions of the VLDL/IDL and HDL fractions and the CE/TC ratio are indicated. A-C: *Statistically significant difference ($P < 0.02$). ApoE, apolipoprotein E; CE, cholesterol ester; FPLC, fast-protein liquid chromatography; LCAT, lecithin cholesterol acyltransferase; LPL, lipoprotein lipase; TC, total cholesterol.

Important differences in the plasma FPLC profiles were observed when mice were infected with 3.5×10^9 pfu of adenovirus expressing either the wild-type or the mutant truncated apoE form four days postinfection. In both cases, the HDL cholesterol peak was reduced, and all cholesterol of the HDL/LDL/IDL/VLDL was unesterified (CE/TC ratio, 0.01 to 0.23) (Fig. 7E, F). In addition, the VLDL/IDL/LDL cholesterol peak of apoE$^{-/-}$ mice expressing apoE4[R142C]-202 was greatly enhanced, and there was a pronounced shoulder of cholesterol spanning the IDL/LDL region (Fig. 7F). This exaggerated phenotype occurs despite the fact that the levels of expression of apoE4[R142C]-202 are lower than those of the WT apoE4-202 (Fig. 7C).

Western blotting of FPLC fractions showed the HDL2 peak and the IDL/LDL shoulder was enriched in apoE, whereas the majority of mouse apoA-I appeared to be in the HDL3 and lipid-free fractions (Fig. 7E, F, lower portion). The residual VLDL peak and the IDL/LDL/HDL2 shoulder produced by the truncated apoE4[R142C]-202 (Fig. 7F) partially explain why the clearance of cholesterol appears to be incomplete in mice infected with adenoviruses expressing this mutant compared with mice expressing apoE4-202 (Fig. 7A, B).

When the apoE$^{-/-}$ mice were infected with 2×10^9 pfu of adenovirus expressing the wild-type or the mutant form of apoE4-202, the residual cholesterol on day 4 was distributed in all lipoprotein classes, the HDL cholesterol was mostly esterified (CE/TC ratio, 0.63 to 0.70) and the VLDL/IDL/LDL cholesterol was mostly unesterified (supplementary Fig. IIA, B). In contrast, the cholesterol of all lipoprotein classes in noninfected apoE$^{-/-}$ mice was mostly esterified (CE/TC ratio, 0.72 to 0.87) (supplementary Fig. IIC).

Density gradient ultracentrifugation of plasma followed by SDS-PAGE analysis of the resulting fractions showed that when mice were infected with 3.5×10^9 pfu of adenovirus expressing apoE4[R142C]-202 or apoE4-202, the major

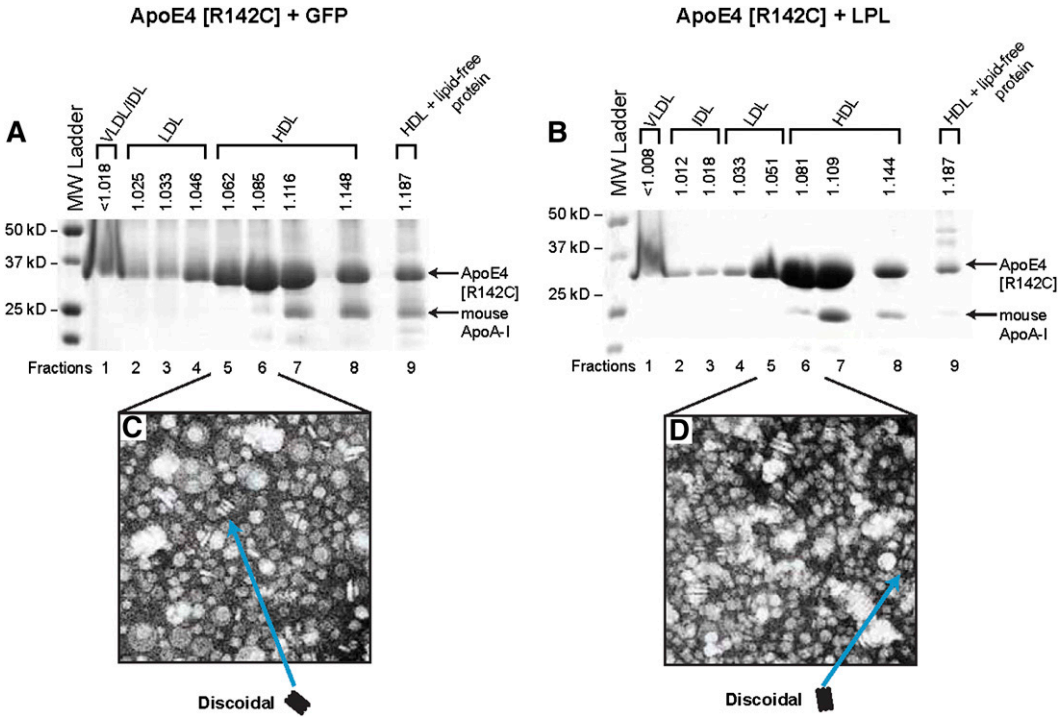

Fig. 6. Distribution of apoE in different lipoprotein fractions following density gradient ultracentrifugation of plasma and EM analysis of HDL fractions. Samples obtained from apoE$^{-/-}$ mice four days postinfection with 7×10^8 pfu adenovirus expressing apoE4[R142C] and 5×10^8 pfu of adenovirus expressing either GFP or LPL were fractionated by density gradient ultracentrifugation and analyzed by SDS-PAGE and EM as described in "Materials and Methods." The density of each fraction and the position of apoE in the VLDL/IDL, LDL, and HDL region are indicated. A, B: SDS-PAGE analysis of lipoprotein fractions derived from mice co-infected with 7×10^8 pfu apoE4[R142C] and (A) 5×10^8 pfu GFP or (B) 5×10^8 pfu LPL. Fractions 5 and 6 were pooled and analyzed by EM. C, D: EM analysis of fractions obtained from apoE$^{-/-}$ mice infected with a mixture of adenoviruses expressing apoE4[R142C] and (C) GFP or (D) LPL. ApoE, apolipoprotein E; EM, electron microscopy; LPL, lipoprotein lipase.

portion of apoE was distributed in the HDL2 region and, to a lesser extent, in the HDL3 region, whereas the endogenous mouse apoA-I was found predominantly in the HDL3 region and the lipoprotein-free fraction (**Fig. 8A**, B). Electron microscopy of the HDL fractions 5 and6 (Fig. 8A, B), which are enriched in apoE, showed the presence of a mixture of discoidal and spherical HDL particles (Fig. 8C, D).

On the basis of the apoprotein composition of the HDL fractions analyzed by EM, the particles originating from apoE4-202 contain both apoA-I and apoE (Fig. 8A), and those originating from the apoE4[R142C]202 mutant contain predominantly apoE (Fig. 8B). Taken together, the findings illustrated in Figs. 7 and 8 demonstrate that the mutant apoE4[R142C]-202 as well as the wild-type apoE4-202 forms have some differences in their lipid and lipoprotein phenotypes when expressed in apoE$^{-/-}$ mice, but they also share two common properties. They are capable of clearing cholesterol without induction of hypertriglyceridemia, and they promote the formation of discoidal HDL particles.

DISCUSSION

Background

A variety of rare apoE mutations between residues 136-147 have been described. These mutations are associated with a dominant inheritance of type III HLP that is manifested at an early age (7, 12).

The importance of the 136-152 region of apoE for binding to the LDL receptor was assessed by in vitro mutagenesis (8, 13, 22). It has been recognized that the binding affinity of these apoE mutants for the receptor observed in vitro did not always correlate with the severity of the dyslipidemia observed in vivo. Thus, it was suggested that the occurrence of the disease can be influenced by other, secondary factors (7, 8, 13, 22–24). These factors may be related to the apoE phenotype, which affects the distribution of apoE to different lipoprotein classes (25, 26), or to the interaction of apoE with heparan sulfate proteoglycans (27).

Heterozygous patients with a dominant form of type III HLP carrying the ε3 allele and a mutant allele were described in 1983 (28). The product of the mutant allele predominated in the plasma of the affected subjects by 3:1 compared with the product of the normal ε3 allele (13). Sequence analysis identified an R142C substitution in the ε4 allele (Arg112 Cys142 Arg158) (29). DMPC proteoliposomes containing the R142C variant expressed in bacteria had reduced binding affinity for the LDL receptor, a receptor blocking monoclonal antibody, and heparin based on competition experiments (13). Unexpectedly, β-VLDL isolated from subjects expressing the apoE4[R142C]mutant showed increased receptor binding affinity based on

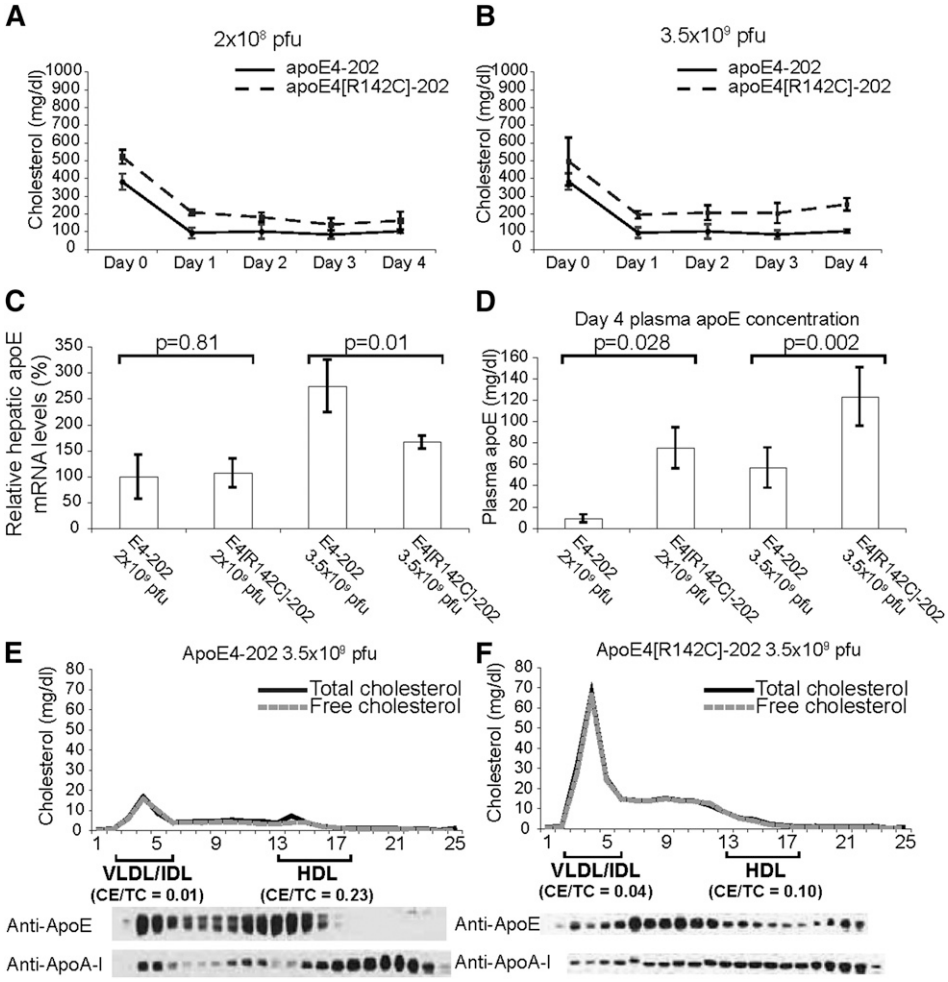

Fig. 7. Plasma cholesterol, triglycerides, apoE, and apoE mRNA levels of apoE$^{-/-}$ mice infected with recombinant adenoviruses expressing apoE4-202 or apoE4[R142C]-202. Plasma lipids were determined days 0, 1, 2, 3, and 4 postinfection. Plasma apoE and apoE mRNA levels were determined day 4 postinfection. A: Plasma cholesterol of mice infected with 2×10^9 pfu of adenoviruses expressing apoE4-202 or apoE4[R142C]-202 (n = 6). B: Plasma cholesterol of mice infected with 3.5×10^9 pfu of adenoviruses expressing apoE4-202 or apoE4[R142C]-202. C, D: Levels of hepatic human apoE mRNA and plasma apoE. E, F: FPLC profiles of total and free cholesterol from apoE$^{-/-}$ mice infected with 3.5×10^9 pfu of adenoviruses expressing (E) apoE4-202 or (F) apoE4[R142C]-202. The positions of VLDL/IDL and HDL fractions as well as the CE/TC ratio are indicated. The distribution of apoE and apoA-I in the different fractions is shown beneath E and F. ApoE, apolipoprotein E; CE, cholesterol ester; EM, electron microscopy; FPLC, fast-protein liquid chromatography; TC, total cholesterol.

competition experiments (23). Several transgenic mouse lines expressing the apoE4[R142C] mutant have been generated and studied. These lines expressed the mutant apoE allele as well as their endogenous mouse apoE gene (30–32). Some of the mouse lines produced a phenotype characterized by mild hypercholesterolemia, hypertriglyceridemia, and very high levels of plasma apoE (30). The β-VLDL obtained from these mice was cleared at a significantly slower rate than normal mouse VLDL (30).

Lipid and lipoprotein phenotype of E$^{-/-}$ mice expressing the apoE4[R142C] mutant

Here we studied the molecular etiology of the dominant dyslipidemia caused by the apoE4[R142C] mutation using adenovirus-mediated gene transfer in apoE$^{-/-}$ mice. The advantage of the adenovirus system is that when the mutant protein is expressed in apoE$^{-/-}$ mice, it creates within a few days the phenotype expected of subjects with homozygous defect in ε4. Human subjects or experimental animals homozygous for the R142C mutation have not been studied previously. Our study provides novel information about the lipid and lipoprotein abnormalities associated with the R142C substitution in apoE4. The phenotype generated by expression of the apoE4[R142C] mutant in apoE$^{-/-}$ mice is much more severe than in transgenic mice that also express the endogenous apoE gene (30). The observed phenotype is characterized by severe hypercholesterolemia and hypertriglyceridemia, reduced CE/TC ratio in different lipoprotein fractions, formation of discoidal apoE-containing HDL, very high plasma apoE levels, and accumulation of apoE in the VLDL/IDL/LDL region. Abnormal lipid and

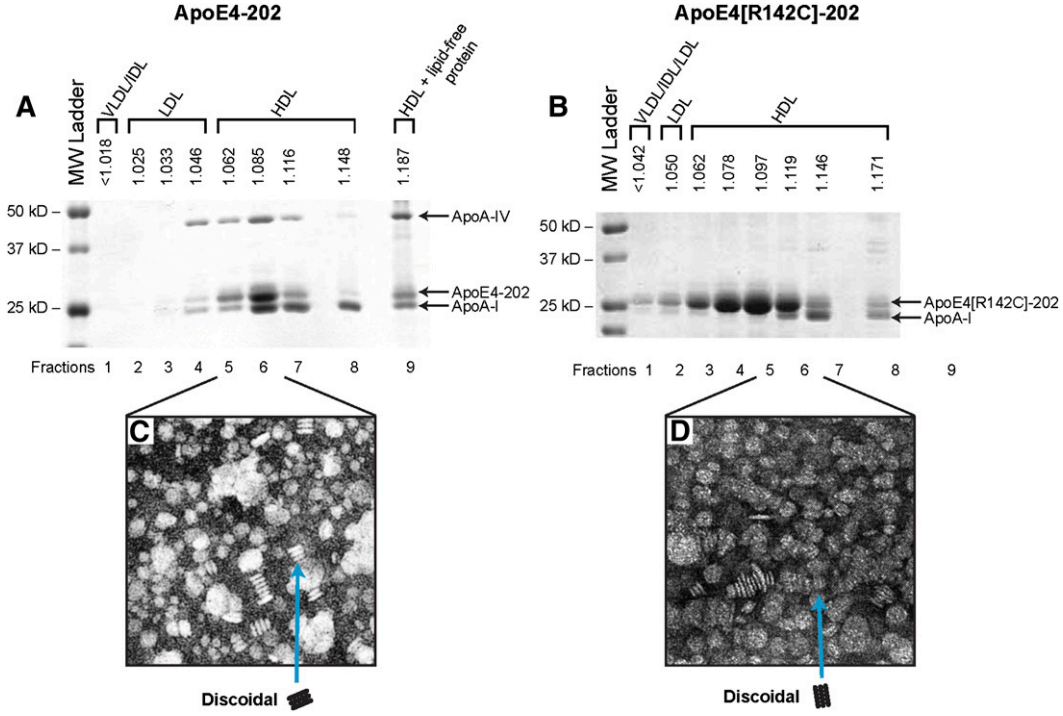

Fig. 8. Distribution of apoE in different lipoprotein fractions following density gradient ultracentrifugation of plasma. A, B: Samples obtained from apoE$^{-/-}$ mice day 4 postinfection with 3.5×10^9 pfu of adenovirus expressing (A) apoE4-202 or (B) apoE4[R142C]-202 were fractionated by density gradient ultracentrifugation and analyzed by SDS-PAGE as described in "Materials and Methods." The density of each fraction and the position of apoE in the VLDL/IDL, LDL, and HDL fractions are indicated. Fractions 5 and 6 were pooled and analyzed by EM. C, D: EM analysis of samples obtained from apoE$^{-/-}$ mice infected with 3.5×10^9 pfu of adenovirus expressing (C) apoE4-202 or (D) apoE4[R142C]-202. ApoE, apolipoprotein E; EM, electron microscopy.

lipoprotein phenotypes have been observed in mice as a result of overexpression of the endogenous mouse apoE (33). Thus the observed dyslipidemia in this study cannot be attributed to abnormal interactions of the human apoE with the mouse apolipoproteins. The phenotype generated by apoE4[R142C] is dominant and persists when the mutant and the WT apoE are co-expressed in apoE$^{-/-}$ mice.

Molecular etiology of apoE4[R142C] dyslipidemia

The accumulation of apoE in the VLDL/IDL/LDL region appears to create insufficiency for both LPL and LCAT activity that can be transiently corrected by co-expression of the mutant apoE and either LPL or LCAT. The insufficiency in LCAT may be explained by fast catabolism by the kidney of LCAT bound to discoidal HDL particles that are formed in the plasma of mice expressing apoE4[R142C]. Accelerated catabolism of discoidal particles and reduction in LCAT activity has been observed in subjects with apoA-I mutations (34, 35). As reported previously (36, 37), the insufficiency of LPL appears to result from inhibition of this enzyme by apoE, which accumulates in VLDL/IDL/LDL-size lipoprotein particles.

The LCAT treatment partially corrected the hypertriglyceridemia and generated spherical HDL particles, but it did not correct the hypercholesterolemia. The LPL treatment, on the other hand, partially corrected the plasma cholesterol levels on day 1 postinfection and the triglyceride levels on days 1–4 postinfection. The increased levels of plasma LPL following gene transfer may promote lipoprotein clearance both by increasing the rate of lipolysis and exposing the receptor-binding domain of apoE, as well as by direct receptor-mediated clearance mechanisms involving LPL (38, 39). Other studies have suggested that excess of secreted apoE may partially displace the LPL and/or apoCII and reduce the rate of lipoprotein triglyceride lipolysis (40, 41). As observed in this study, the ability of excess LPL to partially correct the dyslipidemia induced by apoE4[R142C] suggests that the activity of LPL rather than apoCII may be rate limiting for the clearance of VLDL/IDL/LDL triglycerides. The increased apoE levels are also associated with defective conversion from the discoidal to spherical HDL.

Induction of dyslipidemia requires the C-terminal region of apoE4[R142C]

ApoE contains N-terminal and C-terminal domains that unfold independently (42, 43). The X-ray crystallography of lipid-free apoE isoforms showed that apoE4 is more compact than apoE3 due to differences in domain interactions (44–46). It has been proposed that these interactions may be at least partially responsible for the preferential association of apoE4 with VLDL (25, 45–47) and the contribution of apoE4 to Alzheimer's disease (48).

We recently showed that defective recognition of apoE-containing lipoproteins, either due to mutations in apoE or deficiency in the LDL receptor, may increase the sensitivity and severity of hypertriglyceridemia (49). The same study also showed that the LDL receptor alone can account for the clearance of apoE-containing lipoprotein remnants in mice and that the contribution of the other members of the LDL-receptor family and heparan sulfate proteoglycans (HSPG) may be limited (49).

ApoE4[R142C]-induced dyslipidemia could be the result of altered recognition of the receptor binding domain of the mutant protein by the LDL receptor, as reported previously (13). Alternatively, it could be the result of unfavorable interactions between the N- and C-terminal domains that shield the receptor-binding domain of apoE. Or it could be a combination of both. Our data indicate that full-length apoE4[R142C], despite its abundance in plasma, cannot promote receptor-mediated clearance of apoE-containing lipoproteins in vivo. This finding suggests that the amino terminal portion of the full-length apoE4[R142C] bound to lipoprotein particles assumes a configuration that masks its receptor-binding domain.

The contribution of the C-terminal region of apoE4[R142C] to the induction of dyslipidemia was addressed by gene transfer experiments using the truncated apoE4[R142C]-202 form that extends from residue 1 to 202. The present study showed that, in contrast to the full-length mutant protein, high levels of expression of the truncated apoE4[R142C]-202 form partially corrected the high cholesterol levels of apoE$^{-/-}$ mice without induction of hypertriglyceridemia, indicating that it does not inhibit lipolysis and promotes clearance of the lipoprotein remnants. These findings are consistent with previous studies involving other truncated apoE forms (50). They are also consistent with the previously reported LDL receptor-binding ability of proteoliposomes containing truncated apoE-184 or apoE-191 (51). Expression of the truncated apoE4[R142C]-202 form in apoE$^{-/-}$ mice resulted in increased levels of free cholesterol in the VLDL and formation of a shoulder of cholesterol spanning the IDL/LDL/HDL2 region compared with the truncated wild-type form. This finding explains the partial clearance of cholesterol observed in E$^{-/-}$ mice on days 2–4 postinfection with high doses of the adenoviruses expressing apoE4[R142C]-202 observed (Fig. 7A, B). A common property of the mutant and WT truncated apoE-202 forms is that, at high levels of expression, they also inhibited the esterification of the cholesterol in all lipoprotein fractions and promoted formation of discoidal HDL.

Combined with previous studies, our data indicate that the dyslipidemia induced by E4[R142C] in mice and possibly human patients carrying this mutation is most likely brought about by an altered conformation of the mutant protein bound to the VLDL/IDL/LDL particles that impedes the clearance of triglyceride-rich lipoproteins. The accumulation of apoE in VLDL/LDL/IDL appears to alter the functions of LPL and LCAT, cause hypertriglyceridemia, prevent lipoprotein clearance, and inhibit the maturation of the discoidal into spherical HDL particles. These defects can be transiently corrected by co-expression of apoE4[R142C] with LPL or LCAT. Removal of the carboxy terminal segment of the mutant protein promotes partial clearance of lipoprotein remnants and does not induce hypertriglyceridemia.

REFERENCES

1. Plump, A. S., J. D. Smith, T. Hayek, K. Aalto-Setala, A. Walsh, J. G. Verstuyft, E. M. Rubin, and J. L. Breslow. 1992. Severe hypercholesterolemia and atherosclerosis in apolipoprotein E-deficient mice created by homologous recombination in ES cells. *Cell.* **71:** 343–353.
2. Schaefer, E. J., R. E. Gregg, G. Ghiselli, T. M. Forte, J. M. Ordovas, L. A. Zech, and H. B. Brewer, Jr. 1986. Familial apolipoprotein E deficiency. *J. Clin. Invest.* **78:** 1206–1219.
3. Reddick, R. L., S. H. Zhang, and N. Maeda. 1994. Atherosclerosis in mice lacking apo E. Evaluation of lesional development and progression. *Arterioscler. Thromb.* **14:** 141–147.
4. Herz, J., and T. E. Willnow. 1995. Lipoprotein and receptor interactions in vivo. *Curr. Opin. Lipidol.* **6:** 97–103.
5. Kim, D. H., H. Iijima, K. Goto, J. Sakai, H. Ishii, H. J. Kim, H. Suzuki, H. Kondo, S. Saeki, and T. Yamamoto. 1996. Human apolipoprotein E receptor 2. A novel lipoprotein receptor of the low density lipoprotein receptor family predominantly expressed in brain. *J. Biol. Chem.* **271:** 8373–8380.
6. Takahashi, S., Y. Kawarabayasi, T. Nakai, J. Sakai, and T. Yamamoto. 1992. Rabbit very low density lipoprotein receptor: a low density lipoprotein receptor-like protein with distinct ligand specificity. *Proc. Natl. Acad. Sci. USA.* **89:** 9252–9256.
7. Mahley, R. W., and S. C. Rall, Jr. 2001. Type III hyperlipoproteinemia (dysbetalipoproteinemia): the role of apolipoprotein E in normal and abnormal lipoprotein metabolism. *In* C. R. Scriver, A. L. Beaudet, D. Valle, et al., editors. The Metabolic and Molecular Bases of Inherited Disease. McGraw-Hill, NY. 2835–2862.
8. Rall, S. C., Jr., and R. W. Mahley. 1992. The role of apolipoprotein E genetic variants in lipoprotein disorders. *J. Intern. Med.* **231:** 653–659.
9. Kypreos, K. E., and V. I. Zannis. 2007. Pathway of biogenesis of apolipoprotein E-containing HDL in vivo with the participation of ABCA1 and LCAT. *Biochem. J.* **403:** 359–367.
10. Breslow, J. L., V. I. Zannis, T. R. SanGiacomo, J. L. Third, T. Tracy, and C. J. Glueck. 1982. Studies of familial type III hyperlipoproteinemia using as a genetic marker the apoE phenotype E2/2. *J. Lipid Res.* **23:** 1224–1235.
11. Havel, R. J., and J. P. Kane. 1973. Primary dysbetalipoproteinemia: predominance of a specific apoprotein species in triglyceride-rich lipoproteins. *Proc. Natl. Acad. Sci. USA.* **70:** 2015–2019.
12. Zannis, V. I., D. Kardassis, and E. E. Zanni. 1993. Genetic mutations affecting human lipoproteins, their receptors, and their enzymes. *Adv. Hum. Genet.* **21:** 145–319.
13. Horie, Y., S. Fazio, J. R. Westerlund, K. H. Weisgraber, and S. C. Rall, Jr. 1992. The functional characteristics of a human apolipoprotein E variant (cysteine at residue 142) may explain its association with dominant expression of type III hyperlipoproteinemia. *J. Biol. Chem.* **267:** 1962–1968.
14. Chroni, A., T. Liu, I. Gorshkova, H. Y. Kan, Y. Uehara, A. Von Eckardstein, and V. I. Zannis. 2003. The central helices of apoA-I can promote ATP-binding cassette transporter A1 (ABCA1)-mediated lipid efflux. Amino acid residues 220–231 of the wild-type apoA-I are required for lipid efflux in vitro and high density lipoprotein formation in vivo. *J. Biol. Chem.* **278:** 6719–6730.
15. Liu, T., M. Krieger, H. Y. Kan, and V. I. Zannis. 2002. The effects of mutations in helices 4 and 6 of apoA-I on scavenger receptor class B type I (SR-BI)-mediated cholesterol efflux suggest that formation of a productive complex between reconstituted high density lipoprotein and SR-BI is required for efficient lipid transport. *J. Biol. Chem.* **277:** 21576–21584.
16. Kypreos, K. E., K. W. Van Dijk, Z. A. van Der, L. M. Havekes, and V. I. Zannis. 2001. Domains of apolipoprotein E contributing to triglyceride and cholesterol homeostasis in vivo. Carboxyl-terminal region 203–299 promotes hepatic very low density lipoprotein-triglyceride secretion. *J. Biol. Chem.* **276:** 19778–19786.

17. He, T. C., S. Zhou, L. T. da Costa, J. Yu, K. W. Kinzler, and B. Vogelstein. 1998. A simplified system for generating recombinant adenoviruses. *Proc. Natl. Acad. Sci. USA.* **95:** 2509–2514.
18. Chroni, A., H. Y. Kan, A. Shkodrani, T. Liu, and V. I. Zannis. 2005. Deletions of helices 2 and 3 of human apoA-I are associated with severe dyslipidemia following adenovirus-mediated gene transfer in apoA-I-deficient mice. *Biochemistry.* **44:** 4108–4117.
19. Chroni, A., A. Duka, H. Y. Kan, T. Liu, and V. I. Zannis. 2005. Point mutations in apolipoprotein a-I mimic the phenotype observed in patients with classical lecithin:cholesterol acyltransferase deficiency. *Biochemistry.* **44:** 14353–14366.
20. Li, X., K. Kypreos, E. E. Zanni, and V. Zannis. 2003. Domains of apoE required for binding to apoE receptor 2 and to phospholipids: Implications for the functions of apoE in the brain. *Biochemistry.* **42:** 10406–10417.
21. Fielding, C. J., and P. E. Fielding. 1996. Two-dimensional nondenaturing electrophoresis of lipoproteins: applications to high-density lipoprotein speciation. *Methods Enzymol.* **263:** 251–259.
22. Lalazar, A., K. H. Weisgraber, S. C. Rall, Jr., H. Giladi, T. L. Innerarity, A. Z. Levanon, J. K. Boyles, B. Amit, M. Gorecki, R. W. Mahley, et al. 1988. Site-specific mutagenesis of human apolipoprotein E. Receptor binding activity of variants with single amino acid substitutions. *J. Biol. Chem.* **263:** 3542–3545.
23. Chappell, D. A. 1989. High receptor binding affinity of lipoproteins in atypical dysbetalipoproteinemia (type III hyperlipoproteinemia). *J. Clin. Invest.* **84:** 1906–1915.
24. Hui, D. Y., T. L. Innerarity, and R. W. Mahley. 1984. Defective hepatic lipoprotein receptor binding of beta-very low density lipoproteins from type III hyperlipoproteinemic patients. Importance of apolipoprotein E. *J. Biol. Chem.* **259:** 860–869.
25. Weisgraber, K. H. 1990. Apolipoprotein E distribution among human plasma lipoproteins: role of the cysteine-arginine interchange at residue 112. *J. Lipid Res.* **31:** 1503–1511.
26. Steinmetz, A., C. Jakobs, S. Motzny, and H. Kaffarnik. 1989. Differential distribution of apolipoprotein E isoforms in human plasma lipoproteins. *Arteriosclerosis.* **9:** 405–411.
27. Ji, Z. S., S. Fazio, and R. W. Mahley. 1994. Variable heparan sulfate proteoglycan binding of apolipoprotein E variants may modulate the expression of type III hyperlipoproteinemia. *J. Biol. Chem.* **269:** 13421–13428.
28. Havel, R. J., L. Kotite, J. P. Kane, P. Tun, and T. Bersot. 1983. Atypical familial dysbetalipoproteinemia associated with apolipoprotein phenotype E3/3. *J. Clin. Invest.* **72:** 379–387.
29. Rall, S. C., Jr., Y. M. Newhouse, H. R. Clarke, K. H. Weisgraber, B. J. McCarthy, R. W. Mahley, and T. P. Bersot. 1989. Type III hyperlipoproteinemia associated with apolipoprotein E phenotype E3/3. Structure and genetics of an apolipoprotein E3 variant. *J. Clin. Invest.* **83:** 1095–1101.
30. Fazio, S., Y. L. Lee, Z. S. Ji, and S. C. Rall, Jr. 1993. Type III hyperlipoproteinemic phenotype in transgenic mice expressing dysfunctional apolipoprotein E. *J. Clin. Invest.* **92:** 1497–1503.
31. Fazio, S., Y. Horie, W. S. Simonet, K. H. Weisgraber, J. M. Taylor, and S. C. Rall, Jr. 1994. Altered lipoprotein metabolism in transgenic mice expressing low levels of a human receptor-binding-defective apolipoprotein E variant. *J. Lipid Res.* **35:** 408–416.
32. Fazio, S., K. R. Marotti, Y. L. Lee, C. K. Castle, G. W. Melchior, and S. C. Rall, Jr. 1994. Co-expression of cholesteryl ester transfer protein and defective apolipoprotein E in transgenic mice alters plasma cholesterol distribution. Implications for the pathogenesis of type III hyperlipoproteinemia. *J. Biol. Chem.* **269:** 32368–32372.
33. Drosatos, K., D. Sanoudou, K. E. Kypreos, D. Kardassis, and V. I. Zannis. 2007. A dominant negative form of the transcription factor c-Jun affects genes that have opposing effects on lipid homeostasis in mice. *J. Biol. Chem.* **282:** 19556–19564.
34. Koukos, G., A. Chroni, A. Duka, D. Kardassis, and V. I. Zannis. 2007. LCAT can rescue the abnormal phenotype produced by the natural ApoA-I mutations (Leu141Arg)Pisa and (Leu159Arg)FIN. *Biochemistry.* **46:** 10713–10721.
35. Miettinen, H. E., H. Gylling, T. A. Miettinen, J. Viikari, L. Paulin, and K. Kontula. 1997. Apolipoprotein A-IFin. Dominantly inherited hypoalphalipoproteinemia due to a single base substitution in the apolipoprotein A-I gene. *Arterioscler. Thromb. Vasc. Biol.* **17:** 83–90.
36. Jong, M. C., V. E. Dahlmans, M. H. Hofker, and L. M. Havekes. 1997. Nascent very-low-density lipoprotein triacylglycerol hydrolysis by lipoprotein lipase is inhibited by apolipoprotein E in a dose-dependent manner. *Biochem. J.* **328:** 745–750.
37. Rensen, P. C., and T. J. van Berkel. 1996. Apolipoprotein E effectively inhibits lipoprotein lipase-mediated lipolysis of chylomicron-like triglyceride-rich lipid emulsions in vitro and in vivo. *J. Biol. Chem.* **271:** 14791–14799.
38. Salinelli, S., J. Y. Lo, M. P. Mims, E. Zsigmond, L. C. Smith, and L. Chan. 1996. Structure-function relationship of lipoprotein lipase-mediated enhancement of very low density lipoprotein binding and catabolism by the low density lipoprotein receptor. Functional importance of a properly folded surface loop covering the catalytic center. *J. Biol. Chem.* **271:** 21906–21913.
39. Medh, J. D., S. L. Bowen, G. L. Fry, S. Ruben, M. Andracki, I. Inoue, et al. 1996. Lipoprotein lipase binds to low density lipoprotein receptors and induces receptor-mediated catabolism of very low density lipoproteins in vitro. *J. Biol. Chem.* **271:** 17073–17080.
40. Huang, Y., X. Q. Liu, S. C. Rall, Jr., and R. W. Mahley. 1998. Apolipoprotein E2 reduces the low density lipoprotein level in transgenic mice by impairing lipoprotein lipase-mediated lipolysis of triglyceride-rich lipoproteins. *J. Biol. Chem.* **273:** 17483–17490.
41. Huang, Y., X. Q. Liu, S. C. Rall, Jr., J. M. Taylor, A. Von Eckardstein, G. Assmann, and R. W. Mahley. 1998. Overexpression and accumulation of apolipoprotein E as a cause of hypertriglyceridemia. *J. Biol. Chem.* **273:** 26388–26393.
42. Wetterau, J. R., L. P. Aggerbeck, S. C. Rall, Jr., and K. H. Weisgraber. 1988. Human apolipoprotein E3 in aqueous solution. I. Evidence for two structural domains. *J. Biol. Chem.* **263:** 6240–6248.
43. Aggerbeck, L. P., J. R. Wetterau, K. H. Weisgraber, C. S. Wu, and F. T. Lindgren. 1988. Human apolipoprotein E3 in aqueous solution. II. Properties of the amino- and carboxyl-terminal domains. *J. Biol. Chem.* **263:** 6249–6258.
44. Wilson, C., M. R. Wardell, K. H. Weisgraber, R. W. Mahley, and D. A. Agard. 1991. Three-dimensional structure of the LDL receptor-binding domain of human apolipoprotein E. *Science.* **252:** 1817–1822.
45. Dong, L. M., C. Wilson, M. R. Wardell, T. Simmons, R. W. Mahley, K. H. Weisgraber, and D. A. Agard. 1994. Human apolipoprotein E. Role of arginine 61 in mediating the lipoprotein preferences of the E3 and E4 isoforms. *J. Biol. Chem.* **269:** 22358–22365.
46. Dong, L. M., and K. H. Weisgraber. 1996. Human apolipoprotein E4 domain interaction. Arginine 61 and glutamic acid 255 interact to direct the preference for very low density lipoproteins. *J. Biol. Chem.* **271:** 19053–19057.
47. Weisgraber, K. H. 1994. Apolipoprotein E: structure-function relationships. *Adv. Protein Chem.* **45:** 249–302.
48. Mahley, R. W., K. H. Weisgraber, and Y. Huang. 2006. Apolipoprotein E4: a causative factor and therapeutic target in neuropathology, including Alzheimer's disease. *Proc. Natl. Acad. Sci. USA.* **103:** 5644–5651.
49. Kypreos, K. E., and V. I. Zannis. 2006. LDL receptor deficiency or apoE mutations prevent remnant clearance and induce hypertriglyceridemia in mice. *J. Lipid Res.* **47:** 521–529.
50. Zannis, V. I., A. Chroni, K. E. Kypreos, H. Y. Kan, T. B. Cesar, E. E. Zanni, and D. Kardassis. 2004. Probing the pathways of chylomicron and HDL metabolism using adenovirus-mediated gene transfer. *Curr. Opin. Lipidol.* **15:** 151–166.
51. Lalazar, A., and R. W. Mahley. 1989. Human apolipoprotein E. Receptor binding activity of truncated variants with carboxyl-terminal deletions. *J. Biol. Chem.* **264:** 8447–8450.

ERRATUM

The authors of "Molecular etiology of a dominant form of type III hyperlipoproteinemia caused by R142C substitution in apoE4" (*J. Lipid Res.* 52:45–56) have advised the *Journal* that they inadvertently omitted acknowledging grant support for their work.

The disclosure statement specifying their grant support should have read as follows:

This work was supported by a grant from the National Institutes of Health (HL68216). A. Vezeridis was supported by the National Institutes of Health Predoctoral Training Grant (HL007969).

This information was not included in the initial versions of the online and print article but has been added in the online version after print publication.

DOI 10.1194/jlr.M008409ERR